

TIP TIMING SPECTRAL ESTIMATION METHOD FOR AEROELASTIC VIBRATIONS OF TURBOMACHINERY BLADES

A. Vercoutter^{1,2}, M. Berthillier¹, A. Talon², B. Burgardt², and J. Lardies¹

¹Institut FEMTO-ST - Département de Mécanique Appliquée
24 chemin de l'Épitaphe, 25000 BESANCON, FRANCE
agathe.vercouter@femto-st.fr

²TURBOMECA
Av. Szydlowski, 64511 BORDES CEDEX, FRANCE
arnaud.talon@turbomeca.fr

Keywords: Tip-timing, blade vibrations, turbomachinery, spectral analysis, mistuning, aeroelastic response, rotating measurements.

Abstract: Tip timing method enables spectral analysis of turbomachinery blades in operation. It consists of several sensors mounted on casings which can estimate the vibration of blades by measuring time of arrival of each blade tip. Thus, tip timing is an easy to set up device, as it requires no rotating instrumentation and it is a non intrusive measurement method. Moreover all blades can be monitored; this is very useful for real rotors which always contain a certain amount of mistuning.

We show in this paper how tip timing measurements, processed by a minimum variance estimator can be helpful to analyse and understand aeroelastic phenomenon that can occur on rotors.

1 INTRODUCTION

Blades vibrations, under specific ranges of shaft speeds are usually measured during turbomachinery rig tests. Such measurements are usually made with strain gauges directly positioned on blades, but recently turbomachinery industries have worked on a new measurement method called tip timing because it has multiple advantages. Tip Timing measurement system consists of a set of probes mounted on casings, measuring the passing times of blade tip in front of them (Fig.1). Each probe collects one pulse per revolution and per blade (Fig.2). As the blades are vibrating, these passing times depend on vibrations and shaft speed. Vibration amplitudes can be deduced, as long as shaft speed is known with enough precision. Frequency and amplitude of the vibrations are then estimated in a post processing phase. Thus, tip timing is a non intrusive system which provide information on all the blades whereas strain gauges only measure the instrumented blades. Moreover, as sensors work in the static frame, installation is easier.

However signal analysis is more complicated. As sampling depends on shaft speed and of the number of sensors, sampling frequency is very low compared with the vibrations frequencies. Because the vibration signal is sampled only when the blade is in front of a sensor, it is not possible to apply a low pass filter on original vibration signal and avoid the aliasing effect with traditional spectral estimation. Consequently, different methods have been developed to extract vibratory information from those undersampled data.

We distinguish two kinds of vibration responses to analyse: synchronous vibrations (multiple of shaft speed) and asynchronous vibrations.

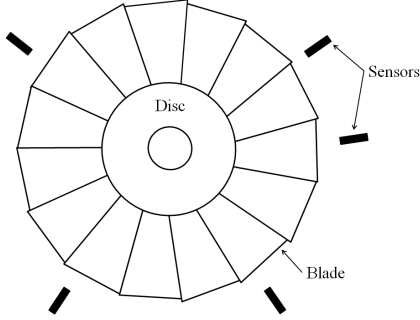


Figure 1: Tip timing on bladed disc

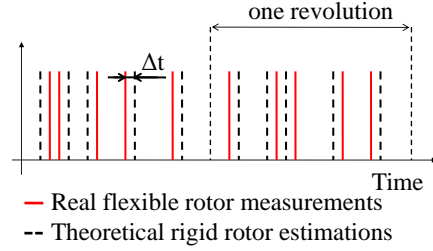


Figure 2: Passing times for one blade in front of the different sensors

Synchronous vibrations are generally analysed with methods based on curves fitting (n parameters sinus fitting, 2 Parameter Plot), autoregressive models (AR, GAR and GARIV) and eigen decomposition (Singular Spectrum Analysis) [1]. These methods all yield engine order estimates and some of them, amplitude estimates. Asynchronous vibrations need to be analysed with spectral estimation methods such as all blade spectrum method [2], the multisampling analysis [3] and the minimum variance spectral estimator [4].

This paper focuses on the application of a minimum variance spectral estimator for asynchronous vibrations. The first part will present the minimum variance algorithm that will be used in this paper. Then this algorithm is applied to analyse asynchronous aeroelastic vibrations measured on a Turbomeca test rig .

2 MINIMUM VARIANCE SPECTRAL ESTIMATOR

We consider number of sensors circumferentially disposed on the stator in front of the blades tip at given axial location. Angular spacing between sensors is usually irregular. The passing times of the blades in front of the sensors is recorded. Knowing the rotation speed, it is possible to deduce the vibration amplitude of each blade, in the rotating frame, at the time it passes in front of each sensor. This reconstructed signal is usually irregularly sampled. Moreover due to the small number of sensors, it is strongly undersampled regarding the blades eigenfrequencies. The minimum variance spectral estimator (MVSE) is then applied to this irregularly undersampled signal.

The MVSE, which was first proposed by Stéphan in the context of tip timing [4], is based on an algorithm developed by Capon [5]. It is a high resolution estimator as it can identify closely spaced peaks. The principle of Capon is based on the minimization of the signal variance to obtain the coefficients of amplitudes in a frequency band. It works as a filter, and is theoretically data independent because it does not adapt to the processed data in any way. Then the user can choose the frequency bandpass.

The power of this filter is equal to

$$E|y(t)|^2 = h^* R h$$

where R is the autocorrelation matrix, y is the sampled signal, h are the coefficients of the filter and $*$ denotes the conjugate transpose.

The method consists in minimizing the total power, subject to the constraint that the filter passes the frequency ω undistorted. This idea can be represented by the following

optimization problem:

$$\min_h h^* R h \quad \text{subject to } h^* a(\omega) = 1$$

where

$$a(\omega) = [1 \quad e^{-i\omega} \quad \dots \quad e^{-im\omega}]^T$$

m is a positive integer, equal to the number of points the signal contains.

The solution of this problem leads to the estimate of the spectral amplitude Y at ω

$$Y(\omega) = \frac{a(\omega)^* R^{-1} y(t)}{a(\omega)^* R^{-1} a(\omega)}$$

It is an iterative algorithm, for each step, the autocorrelation matrix is computed with the Wiener-Khintchin theorem. This theorem links the autocorrelation function and the power spectral density (PSD). The PSD is obtained from the spectral amplitudes computed in the last step (the first PSD can be computed with a non-uniform discrete Fourier transform, NDFT).

Power Spectral Density \Rightarrow Autocorrelation matrix \Rightarrow Spectral amplitude

Convergence is obtained when relative error between the last two PSD is less than 5 percent. This algorithm is statistically stable and gives good results in terms of frequencies.

An example of a signal with three sinusoids and white noise is given. The frequencies are 15Hz, 22Hz and 32 Hz, for the respective amplitudes 10, 4 and 7. The signal to noise ratio is equal to 20. According to the Shannon theorem, a correct sampling frequency should be at a minimum of 64Hz. In this example the signal is sampled with a 10Hz periodic irregular pattern of three points, which approximately corresponds to a mean sampling frequency equal to 30Hz. Ninety points are treated in this example. It reproduces the situation of three non-equispaced sensors recording passing times of a blade under a rotation speed equal to 10Hz and during thirty revolutions of the blade. Figure 3 displays the signal sampled at 70Hz and the points that tip timing system records.

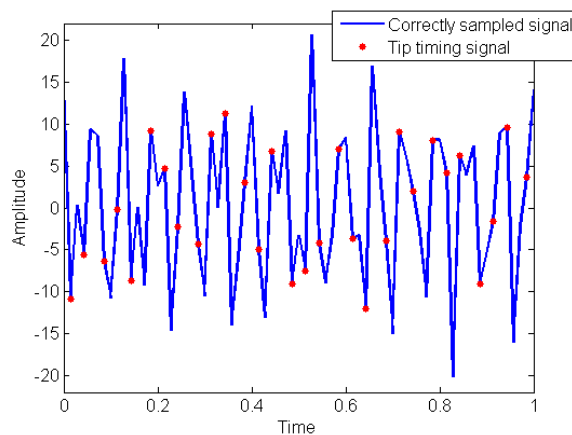


Figure 3: Comparison of signal sampled at 70Hz and tip timing measurements

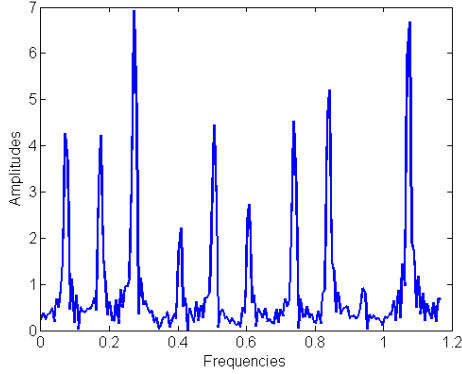


Figure 4: Spectrum after a non-uniform discrete Fourier transform (NDFT)

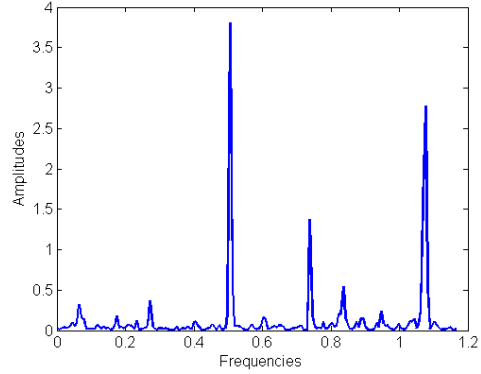


Figure 5: Final spectrum obtained with MVSE (last iteration)

Figure 4 presents the spectrum obtained with the NDFT which corresponds to the first data the MVSE treats and figure 5 presents the final spectrum obtained with the MVSE once it converged. The frequencies were normalized relatively to the mean sampling frequency ($F_s = 30Hz$). It illustrates the capability of the MVSE to compute a spectrum over a large frequency band (in this example from $-1.2 \times F_s$ to $1.2 \times F_s$) compared to the one computed with a simple Fourier transform (from $-0.5 \times F_s$ to $0.5 \times F_s$). Then the three sinusoids whose frequencies are 15Hz, 22Hz and 32Hz can be identified at respective normalized frequencies (N_f) 0.5, 0.73 and 1.07.

The NDFT spectrum (Fig.4) presents some peaks at multiple frequencies. Several of them are artefacts whereas the physical frequencies are clearly visible. The Parseval theorem is respected, which means the total energy of the signal is conserved from the temporal representation to the spectral estimation.

$$E = \int_{-\infty}^{+\infty} |x(t)|^2 dt = \int_{-\infty}^{+\infty} |X(f)|^2 df$$

In the final spectrum computed with MVSE (Fig.5), all the peaks decreased comparing to the NDFT spectrum, especially the artefacts with a ratio greater than 10. The three physical frequencies are now clearly visible, their amplitudes are lower than in the original signal with an average ratio equal to 2.6. The relative amplitudes between the physical peaks are conserved. The MVSE does not respect the Parseval theorem, the total energy decreased with a ratio equal to 3.7.

As a conclusion of this typical example it seems that the MVSE gives correct frequencies but amplitudes must be considered comparatively against each other.

3 INDUSTRIAL TEST CASE ANALYSIS

We will now analyse test rig data recorded at Turbomeca. This analysis intends to identify asynchronous vibrations occurring during the test. The aim of this test is to analyse each blade response in the rotating frame, and identify the spatial organisation of main responses. Generally, the All Blade Spectrum is used in the case of asynchronous vibrations, as it can yield spatial informations. But in that specific case it is not recommended because the main assumption of such estimator, is a well-tuned blade assembly. Therefore data were treated with the Minimum Variance Spectral Estimator, which presents

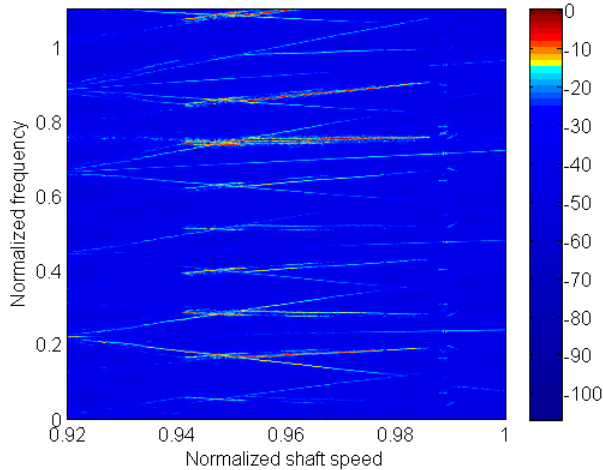


Figure 6: Campbell diagram, computed on one blade, after a NDFT

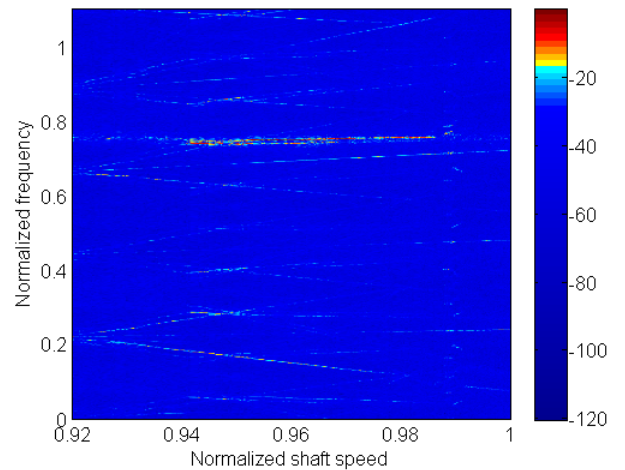


Figure 7: Campbell diagram, computed on one blade (MVSE last iteration)

the interest of focusing on each blade and separating their behavior. Furthermore it works easily with rotor data and can also yield spatial organisation computing a spatial Fourier decomposition.

The compressor rotation is following an accelerating slope. Rotor speed is assumed constant for each measurement group of points on which the MSVE algorithm is applied. In reality rotor speed changes during one rotation, but this hypothesis can be made because the acceleration is slow.

The first diagram of interest is the Campbell diagram (Fig.7) because it gives a global point of view of the test and separate vibrations per frequencies at given rotor speeds. As the shaft speed is accelerating, the Campbell diagram represents vibrations over a range of normalized rotor speeds (N_s) from 0.92 to 1. In this test, as we have five sensors, the equivalent sampling frequency is equal to $\frac{5 \times \Omega_{rot}}{2\pi}$.

Frequencies were normalized with the same method as in the example (Fig.4 and Fig.5). The mean sampling frequency used corresponds to the minimum rotation speed. Amplitudes and rotation speed were normalized relatively to their respective maximums. On the Campbell diagrams, amplitudes are displayed in dB.

The comparison of figures 6 and 7 shows that artefacts due to the computation were reduced during the convergence of the algorithm. The final Campbell diagram still contains artefacts (Fig.7), but one dominant frequency band (called band A) can be identified around a mean normalized frequency $N_f = 0.75$. In fine MVSE algorithm can easily reduce artefacts coming from undersampled data, the physical information included into the spectra arises from aliased contents.

The analysis will focus on the frequency band A, corresponding to blade modal response. Figure 8 displays the Campbell diagram centered on band A. Figure 9 represents the evolution of the normalized amplitude spectrum in the frequency band A as a function of the rotor speed. We can see that an asynchronous vibration is initiated after $N_s = 0.94$, fully developed before $N_s = 0.96$ and disappears after $N_s = 0.99$.

The analysis will pursue identifying spatial organisation of the vibration during two periods: $N_s = 0.92$ to 0.94 and $N_s = 0.94$ to 0.99 . The compressor mistuning makes difficult the use of an all blade spectrum. This particularity is illustrated by figure 10 which

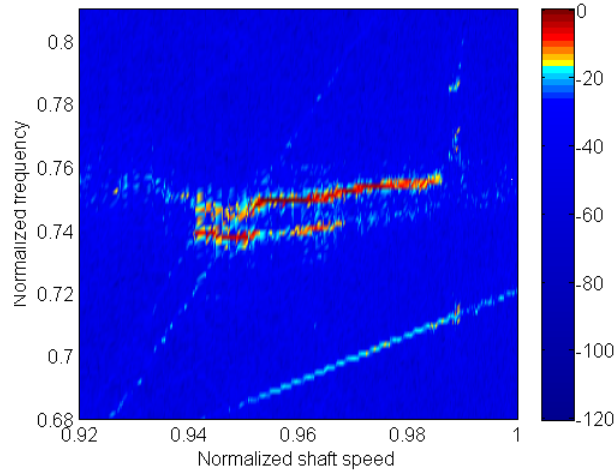


Figure 8: Campbell diagram centered on frequency band A

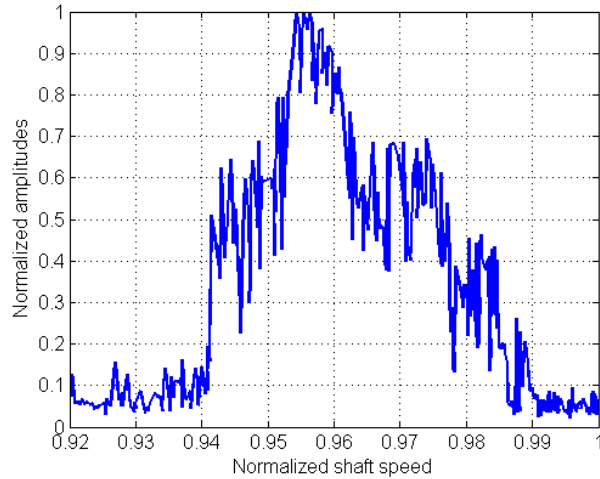


Figure 9: Amplitude of one blade on band A

displays the responses of the maximum and the minimum amplitude blades. Important amplitude differences are visible for the speed range $N_s = 0.94$ to 0.99 , in which mistuning plays an important role.

Investigation on spatial organisation starts by specifying the frequencies of interest at given normalized speeds $N_s = 0.945$, 0.968 and 0.977 . Figure 11 displays the spectrum of the ten first blades of the compressor at $N_s = 0.945$ on the frequency band A. We can identify two frequency peaks for which the vibration of all blades is maximum for the same frequency value. This is typical of an organized vibration on the rotor, probably due to an aeroelastic instability. In contrast, above $N_f = 0.742$ exists a small frequency band in which we can see the superposition of various mistuned responses.

The same plot is made at normalized speeds $N_s = 0.968$ and 0.977 and is represented on figures 12 and 13. Progressively as the rotation speed increases, the organized vibrations dominate. This confirms the hypothesis of an aeroelastic instability. The spatial Fourier transform for the three previous rotation speeds and for the frequencies corresponding to the organized vibrations are presented on figures 14 and 15. The plots are limited to the most interesting wave numbers. Positive wave numbers represent waves rotating in the

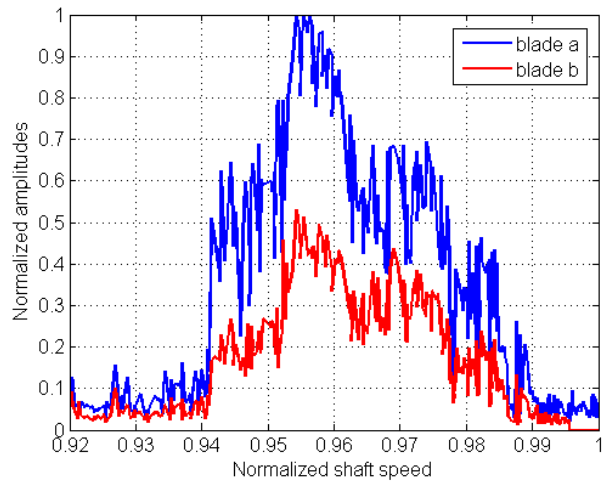


Figure 10: Maximum and minimum amplitude blades

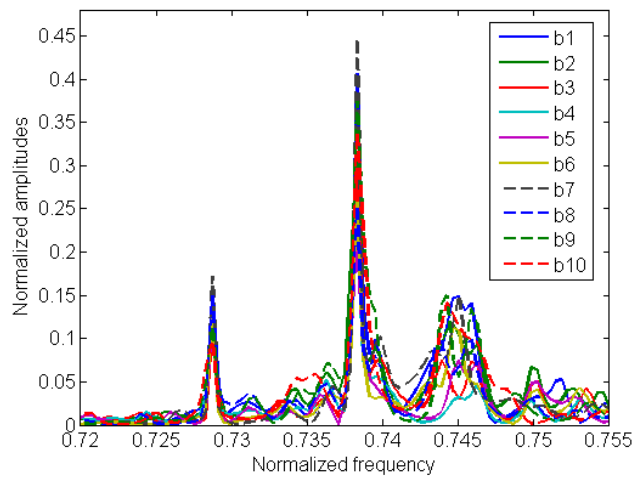


Figure 11: Amplitude spectrum of the ten first blades at $N_s = 0.945$

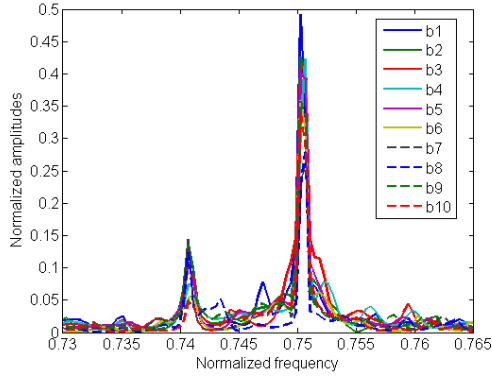


Figure 12: Amplitude spectrum of the ten first blades at $N_s = 0.968$

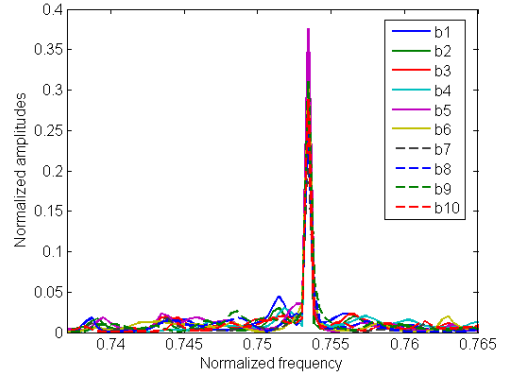


Figure 13: Amplitude spectrum of the ten first blades at $N_s = 0.977$

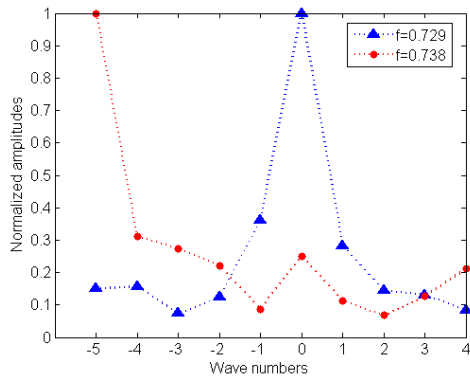


Figure 14: Spatial organisation per frequency at $N_s = 0.945$

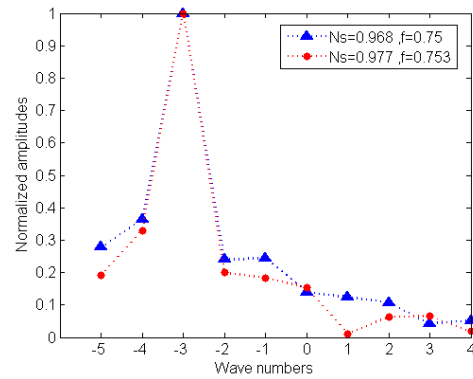


Figure 15: Spatial organisation on principal frequency at $N_s = 0.968$ and 0.977

direction of the rotation. The wave number modulus is equal to the number of the nodal diameters of the vibrations. We can see that the instability is initiated at $N_s = 0.945$ with the wave numbers 0 and -5. Then when it is fully developed, the wave number changed to -3 and remains constant as we can see on the plot for $N_s = 0.968$ and 0.977 . Figure 16 shows the bladed disk pattern at $N_s = 0.977$ and $N_f = 0.753$.

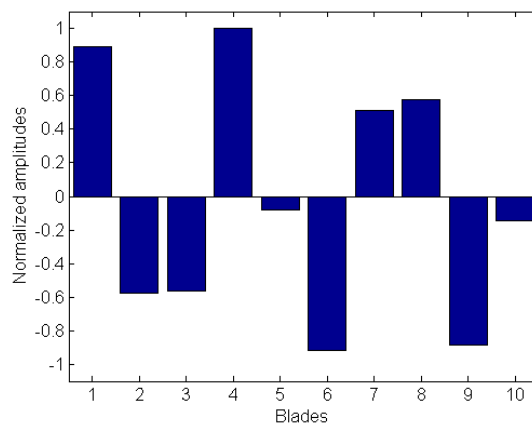


Figure 16: Blades pattern at $N_s = 0.977$ and $N_f = 0.753$

4 CONCLUSION

We presented the Minimum Variance Spectral Estimator for the analysis of tip timing data. We demonstrate the capability of such algorithm to deal with undersampled and aliased data. With this method, aliases are reduced in amplitude that allow to estimate properly physical responses of blade, moreover we can also estimate frequency content beyond the equivalent Shannon frequency.

Those capabilities were demonstrated on a simulated test case and on real data coming from an industrial test rig. This spectral estimation leads to an individual analysis of each blade in the rotating frame.

By estimating spectra on all blades, we can perform a spatial Fourier transform that gives the wave numbers of the phenomenon. We can precisely estimate the mistuned behavior of the rotor in this particular case of an aeroelastic instability.

5 REFERENCES

- [1] Carrington, I. B. (2002). *Development of Blade Tip Timing Data Analysis Techniques*. Ph.D. thesis, School of engineering, University of Manchester.
- [2] Zielinski, M. and Ziller, G. (2000). Noncontact vibration measurements on compressor rotor blades. *Measurement Science and Technology*, 11, 847–856.
- [3] Beuseroy, P. and Lengellé, R. (2007). Nonintrusive turbomachine blade vibration measurement system. *Mechanical Systems and Signal Processing*, (21), 1717–1738.
- [4] Stéphan, C., Berthillier, M., Talon, A., et al. (2008). Tip-timing data analysis for mistuned bladed discs assemblies. GT2008-50825. Berlin, Germany: ASME.
- [5] Stoica, P. and Moses, R. (2005). Capon method, Filter-Bank methods. In *Spectral Analysis of Signals*. Pearson Prentice Hall, pp. 232–238.